ORIGINAL PAPER

Investigation of the structure and tensile strength of ultrahigh molecular weight polyethylene and amide functionalized single-walled carbon nanotubes nanocomposites

Yahia F. Makableh[1] · **Ayat Bozeya**[1] · **Ibrahim Alnasra**[1] · **Tariq Rawshdeh**[1] · **Haneen Abu Hammam**[2]

© The Author(s), under exclusive licence to Springer-Verlag GmbH Germany, part of Springer Nature 2023

Abstract

In this work, the surface of single-wall carbon nanotubes (SWCNTs) was functionalized with amide group to improve the interfacial adhesion and dispersion of the SWCNT within an ultrahigh molecular weight polyethylene (UHMWPE) polymer matrix. The UHMWPE/SWCNTs nanocomposites were prepared by ultra-sonication mixing and hot press molding methods. Fourier transform infrared spectroscopy results confirm the amide functionalization. The prepared nanocomposites were characterized based on morphology, structure, and mechanical properties by scanning electron microscopy, X-ray diffraction, and a Universal Testing Machine, respectively. The crystallinity, crystal size, space between atomic lattice and lattice constant were calculated from XRD spectra. The results show an increase in the UHMWPE crystallinity when adding pristine SWCNTs and Amide-SWCNTs (1–5 wt %) due to changing the nucleation type of the UHMWPE from homogeneous to heterogeneous nucleation, which led to accelerating the nucleation process and the formation of more crystalline grains. The tensile test results show an increase in toughness of ~ 95% when adding 4 wt % Amide-SWCNTs. This indicates that the amide group achieved good interfacial adhesion and dispersion compared to pristine SWCNTs.

Keywords Nanocomposite · UHMWPE · Pristine SWCNTs · Amide-SWCNTs · Dispersion · Interfacial adhesion · Crystallinity

✉ Yahia F. Makableh
  yfmakableh@just.edu.jo

1   Institute of Nanotechnology, Jordan University of Science and Technology, Irbid, Jordan

2   Chemical Engineering Department, Jordan University of Science and Technology, Irbid, Jordan

Introduction

Due to the structure of the bonds possessed by polymeric materials, their importance has increased in recent years due to the low production costs, lightweight, and high mechanical strength [1]. Ultrahigh molecular weight polyethylene (UHMWPE) can be defined as a thermoplastic, linear, unbranched, and semi-crystalline polymer. This polymer is a polyethylene family member as it has an extremely large molecular weight and a very long chain [2, 3]. The molecular weight of UHMWPE is not less than 1 million g/mole with a degree of polymerization of ~ 36,000 according to the International Standards Organization (ISO), while according to the American Society for Testing and Materials (ASTM), UHMWPE has a molecular weight greater than 3.1 million g/mole with a degree of polymerization ~ 110,000 [3]. Single-wall carbon nanotubes (SWCNTs) can be described as a single layer of graphite (graphene layer) rolled into a seamless cylindrical shape. Generally, SWCNTs consist of two separate regions, the sidewall, and the cap of the tube; which contains six pentagonal like one-half of fullerene molecules. These two regions have different physical and chemical properties [4, 5]. SWCNTs have a diameter in the range of (0.3–100) nm, and an average lengths as few micrometers [5]. One of the main challenges in preparing nanocomposites of carbon nanostructures (CNTs) within a polemic matrix is the dispersion between the two materials, and the agglomeration that occurs to the carbon nanostructures. Hence, obtaining a nanocomposite with a certain required properties can be achieved by better dispersion of the filler materials within the polymer matrix, and thus, enhancing the load transfer efficiency applied to the nanocomposite compared to the pristine polymer. One of the main reasons to reach enhanced polymer properties is the high surface to volume ratios that the nanoscale materials possess, thus, increasing the efficiency of the interaction between the two phases of the mixed materials. This ratio controls the interfacial region (interaction zone) that is responsible for creating a new structure on the molecular level, which can improve the transfer efficiency of the loads applied to the composite and thus improve the properties of the nanocomposite [6–9]. Unfortunately, due to the unreactive nature of SWCNTs (strong agglomerates as a result of Vander walls forces), there is no good interfacial interaction between pristine SWCNTs and the UHMWPE matrix [10, 11]. The reason for the poor interaction of the carbon nanotubes with the polymeric matrix is the aromatic nature of the bond that makes the carbon atoms on the carbon nanotubes' surface chemically inert. Functionalization of the carbon nanotubes plays an important role in improving the dispersion and interfacial adhesion between the carbon nanotubes and the polymeric matrix because the hydrophobic nature of the carbon nanotubes changes to hydrophilic due to the polar group attachment [10]. Several studies involving the use of different materials and functional group were used to disperse SWCNTs within a UHMWPE matrix and study its effect on the structure and mechanical properties of UHMWPE/SWCNTs nanocomposite. Zhang et al. oxidized SWCNTs by using three types of oxidants, 1. nitric acid (2.6 M) 2. a mixture of sulfuric (98%) and nitric acid (16 M) with volume ratios

(3: 1), and 3. KMNO$_4$. The oxidation process was characterized by Fourier transform infrared spectroscopy (FTIR) and scanning electron microscope (SEM). The results showed that the use of different oxidants led to the formation of different functional groups on the surface of the SWCNTs [12]. Gromov et al. prepared SWCNT-NH$_2$ by preparing covalent amino-functionalization of SWCNTs. This method involved oxidation of SWCNTs and the production of a carboxyl group on the edge-terminal of the SWCNTs, then chemically transforming it into a SWCNTs- NH$_2$ linked directly on the open ends of the tubes. Successful functionalization steps were characterized by SEM, FTIR, Raman spectroscopy, and X-ray photoelectron spectroscopy (XPS) [13]. Guo et al. studied the crystallization of UHMWPE doped with carbon nanotubes. The degree of crystallinity was investigated by using X-ray diffraction (XRD), where the results showed a significant increase in the crystallinity (71.95–82.92%) of UHMWPE/CNTs composites compared to pristine UHMWPE. This increase is due to changing the nucleation type of UHMWPE from the homogeneous to the heterogeneous nucleation, which led to accelerating the nucleation process and the formation of more crystalline grains [14]. Additionally, Brain et al. mixed UHMWPE powder with 93% Silica and 7% SWCNTs by compression molding with high pressure and temperature. The results showed a significant decrease in mechanical properties in terms of modulus, elongation at break and tensile strength due to the fact that the mixture of SWCNTs/Silica showed a weak interaction [15]. Khatiwada et al. prepared a composite of epoxy/UHMWPE reinforced with 0.5 wt % SWCNTs and used them as bumper shields and as rear walls in Whipple shield configurations at impact velocities. The results showed that the addition of SWCNTs to the composite did not show a significant effect due to lack of functionalization of SWCNTs, which led to weak dispersion within the polymer matrix [16]. Hulsey et al. prepared UHMWPE/SWCNTs nanocomposite by solution spinning. The surface of the SWCNTs was modified by wrapping the polyvinylpyrrolidone (PVP) around the SWCNTs (non-covalent functionalization). The results showed a significant improvement in the mechanical properties of the modified SWCNTs compared to pristine SWCNTs [17]. Also, Khan et al. prepared HUMWPE filaments/2 wt % SWCNTs by solution spinning method. Through the tensile test, the results showed that the addition of 2 wt % of SWCNTs led to a significant improvement in tensile strength and Young's modulus by 120 and 463%, respectively. While there was a clear decrease in the strain at failure when adding SWCNTs to the polymeric matrix [18].

In this work, polymeric matrix nanocomposites were prepared. UHMWPE was used as a polymeric matrix material, with Amide functionalized SWCNTs (Amide-SWCNTs) as reinforcing material with different percentages (1–5 wt %). SWCNTs were oxidized and chemically functionalized with amide group in the first step. Then, the Amide-SWCNTs were dispersed within the UHMWPE matrix to prepare the nanocomposite. The nanocomposite preparation method combines different techniques in order to achieve the intended composites by using ultra-sonication mixing and hot press molding methods. Structural, morphological and mechanical (tensile strength) properties of the prepared nanocomposites sheets were investigated. Up to the authors knowledge, few articles found in the literature are discussing both,

the structural and mechanical properties of UHMWPE nanocomposites in the same time; and for the first time to use the combined preparation methods. It is noted that using the proposed combined preparation methods can highly enhance different properties of the UHMWPE when compared to the pristine polymer. In addition to the enhanced crystallinity of the polymer, the mechanical properties were highly enhanced in the order of 95% for the nanocomposite that has 4% SWCNTs. Moreover the Amide group achieved good interfacial adhesion and dispersion compared to pristine SWCNTs.

Experimental

Materials

The following materials were used without further purifications, single-walled carbon nanotubes (1.3–2.3 nm in diameter, > 70% carbon as SWCNTs, ultrahigh high molecular weight polyethylene; with average molecular weight $(3–6 \times 10^6$ g/mol) and density of 0.94 g/ml, sulfuric acid (H_2SO_4) 98 wt %, N,N-Dimethyl Formamide (DMF) (C_3H_7NO), ethylenediamine anhydrous 99.0% $(C_2H_4(NH_2)_2)$, tetrahydrofuran, oxalyl chloride $(C_2O_2Cl_2) \geq 99\%$, and ethanol anhydrous 91% (C_2H_5OH) were from Sigma Aldrich. Nitric acid (HNO_3) 70 wt % was from SDFCL fine—chem limited.

Methodology

Oxidation of SWCNTs

Pristine single-walled carbon nanotubes (P-SWCNTs) were oxidized by wet chemical oxidation method though using different types of acids. The P-SWCNTs were dispersed into a concentrated mixture of sulfuric (98 wt %) and nitric acid (69 wt %) with a volume ratio (1:3 (vol/vol) sulfuric/nitric). The mixture was then placed in a reflux system with magnetic stirring at 70 °C for 24 h in order to form a carboxylic group on the P-SWCNTs surface (SWCNTs-COOH). The resulted SWCNTs-COOH were diluted by adding distilled water and filtered through cellulose membranes (0.45 µm diameter). The filtrate was washed with distilled water until the pH reached a neutral value (~7) to remove the residual acids and dry at room temperature for 24 h.

Amide functionalization of SWCNTs

Amide-SWCNTs were prepared, as shown in Fig. 1 below; where N,N-Dimethyl Formamide (DMF) was added to SWCNTs-COOH and then sonicated for 1 h. This step was done to obtain a homogenous suspension. Oxalyl chloride was added dropwise to the suspension of the SWCNTs-COOH at 0 °C for 1 h under nitrogen flow to break the OH bond and replace it with Cl; in order to obtain SWCNTs-COCl.
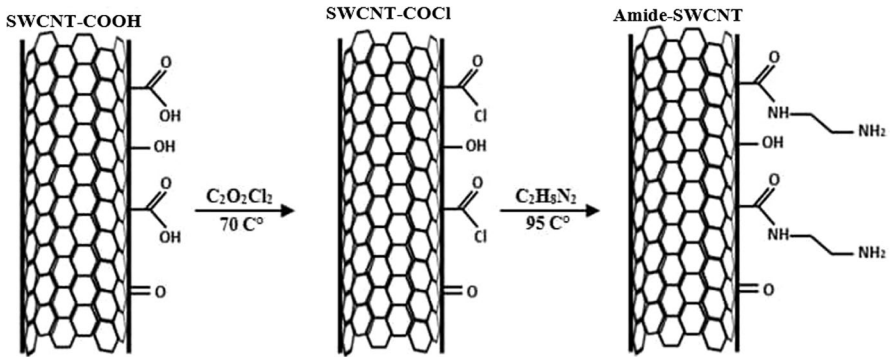
Fig. 1 Schematic diagram showing the mechanism for preparing Amide-SWCNTs

The mixture was stirred for 24 h at 70 °C to remove the excess oxalyl chloride. The amide group was formed by adding ethylenediamine dissolved in DMF to the suspended SWCNTs-COCL and stirring the mixture at 95 °C for three days. Finally, the mixture was cooled to room temperature, filtered, and washed thoroughly with DMF, ethyl alcohol, and tetrahydrofuran (THF), and then dried at room temperature for 24 h.

Preparation of UHMWPE/SWCNTs nanocomposites

UHMWPE/SWCNTs nanocomposites were prepared by dispersing the P-SWCNTs, or Amide-SWCNTs in ethanol with probe sonication for 3 min [19]. Then, UHMWPE was added and sonicated for another 3 min. After this step, the mixture was heated at a temperature of 70 °C with a magnetic stirrer to evaporate the ethanol and to obtain a uniform powder mixture. After the ethanol evaporation, the UHMWPE/SWCNTs powder was dried in an oven at 100° C for 24 h. The resulting sample was compressed by a hot press between two heated panels, one of the panels fixed and the other was moving. The prepared UHMWPE/SWNCTs powder was placed in a mold consisting of two stainless steel plates. Between the two plates, there is a square plate containing the dogbone shape mold, the samples were then pressed at 240 °C and 160 kg/cm^2 for 30 min. After this process was completed, the UHMWPE/SWCNTs nanocomposites were formed, then they were cooled down to room temperature, opened, and the prepared shapes were removed to form the final dogbone shaped sheets as shown in Fig. 2. Table 1 summarizes the composition of the prepared nanocomposites.

Characterization of the UHMWPE/SWCNTs nanocomposites

In this work, scanning electron microscopy images were taken by QUANTA FEG 450, Thermo scientific, Germany, the samples were first sputtered with Gold ~ 10 nm thickness to enhance the images quality. Fourier transform infrared spectroscopy was performed on a Bruker Vertex 80, over the range 5000–400 cm^{-1}. The resolution of

Fig. 2 The prepared dogbone shapes samples by using compression molding for **a** pristine UHMWPE and **b** representative sample of the UHMWPE/SWCNTs nanocomposite
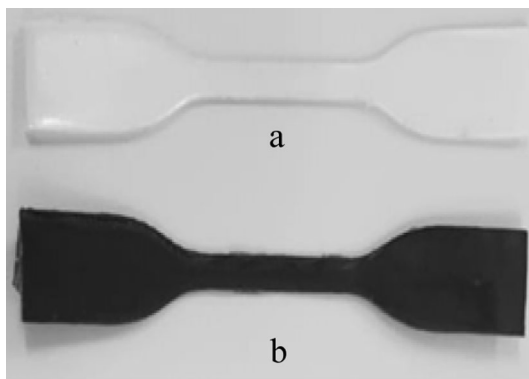

Table 1 Compositions of the prepared UHMWPE/SWCNTs nanocomposites

Sample	Type of SWCNT	% of SWCNT	Polymer	Nanocomposite
S1	–	–	UHMWPE	UHMWPE
S2	P-SWCNTs	1	UHMWPE	UHMWPE/P-SWCNTs
S3	Amide-SWCNTs	1	UHMWPE	UHMWPE/1% Amide-SWCNTs
S4	Amide-SWCNTs	2	UHMWPE	UHMWPE/2% Amide-SWCNTs
S5	Amide-SWCNTs	3	UHMWPE	UHMWPE/3% Amide-SWCNTs
S6	Amide-SWCNTs	4	UHMWPE	UHMWPE/4% Amide-SWCNTs
S7	Amide-SWCNTs	5	UHMWPE	UHMWPE/5% Amide-SWCNTs

the FTIR spectrophotometer was set to 4.0 cm^{-1}, with a total of 32 scans. X-ray diffraction was used at 2θ scanning range of $(3–60)°$ with a step size of $0.02°$, the XRD is equipped with a Cu Kα X-ray tube operated at a 40 kV and 20 mA gun. The scanning speed was set to 3.000 deg/min. DSC 204 F1 Phoenix NETZCH instrument was used for the thermal properties characterization. The samples were heated from room temperature to 200 °C at a rate of 10 °C / min, and then, the samples were cooled to room temperature at the same rate in the presence of N_2 gas flow (20 ml/min.–70 ml/min.). The tensile test was performed on a universal testing machine (BESMAK Material Testing), in which five trials were conducted for each nanocomposite sample. A standard punch (ASTM D-638-IV) was used to prepare the dogbone specimen tensile test. The maximum load was set to 220 N. The specimen was carried out at a cross-head of 5 mm/min.

Results and discussion

FTIR results

The SWCNTs structures were characterized by FTIR spectroscopy. Figure 3 shows the FTIR spectra of P- SWCNTs, oxidized (SWCNTs-COOH), and amide
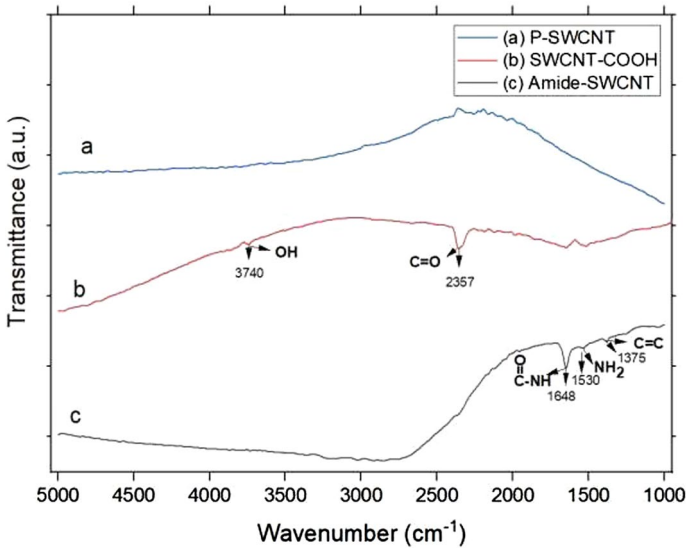
Fig. 3 The FTIR spectra for the **a** P-SWCNTs, **b** SWCNTs-COOH, and **c** Amide-SWCNTs

functionalized structures. The results show the formation of the carboxyl group (COOH) on the surface of the SWCNTs as a result of the emergence of the carbonyl group (C=O) band at peak region 1658.45 cm^{-1} and the hydroxyl group (OH) at peak region 3740 cm^{-1}, respectively, resulting from the stretch vibrations. Furthermore, a strong peak appeared at 2360.43 cm^{-1} that is related to the formation of OH group stretch due to strong nitric acid usage as shown in Fig. 3 for the SWCNT-COOH. This result is in agreement with other published reports [20, 21]. From the same figure and looking at the Amide-SWCNTs curve, it is a noted that shift in the C=O group range from 1654 to 1648 cm^{-1} and the formation of NH$_2$ group at 1530 cm^{-1} as a result of the formation of the amide group. Moreover, the emergence of a peak region at 1375 cm^{-1} can be attributed to the bending vibrations of the C=C group [22].

SEM morphology results

Figure 4 shows the SEM images of the P-SWCNTs and Amide-SWCNTs, while Fig. 5 shows the SEM images for the pure UHMWPE, UHMWPE/P-SWCNTs, and UHMWPE/Amide-SWCNTs (1–5 wt %). It is clearly shown that the P-SWCNTs appeared as bundles of aggregates, which can be explained due to the high Van-der walls force between the CNTs due to the presence of the π-π bonding at the CNTs wall surface Fig. 4(1). Amide functionalization of the SWCNTs decreases the π-π interaction, and hence increase the dispersion of the CNTs (Fig. 4 (2)). In the polymer matrix nanocomposites, it is highly important to have the nanofiller as dispersed as maximum as could be, to enhance the interfacial interaction between the
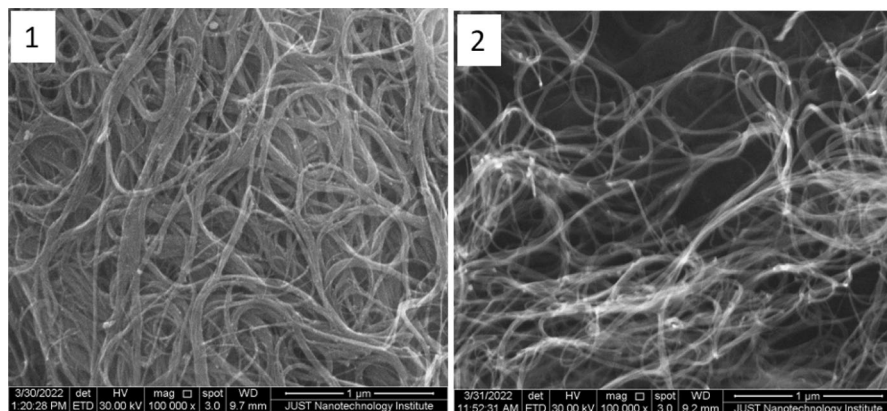
Fig. 4 SEM images for the pristine and Amide functionalized SWCNT, 1: P-SWCNT, 2- Amide-SWCNT

matrix and the nanofiller to enhance the load transfer properties. Using the proposed combined preparation method with the amide functionalization at the surface of the SWCNTs enhances the interfacial adhesion and dispersion of the these modified SWCNTs within the UHMWPE matrix. The results show that there is a clear adhesion of the SWCNTs within the polymer matrix. It can be seen that P-SWCNTs were dispersed in the form of agglomerates within the UHMWPE matrix resulting from the Van der Waals forces Fig. 5a, b, while the Amide-SWCNTs appeared to have less aggregates and more dispersed within the matrix up to 4%. However, aggregates formed at higher percentage 5% are clearly shown in Fig. 5m, n; this is due to the high percentage of the filler, and the high surface energy of the CNTs that tend to agglomerate to decrease the surface energy. At higher percentages, the CNTs are present as aggregates within the polymer matrix with reduced agglomerations. Hence, they had good dispersion within the UHMWPE matrix, especially when 4 wt % Amide-SWCNTs were added. It can also be observed that there is a clear agglomeration occurs when adding 5 wt % Amide-SWCNTs to the polymer matrix.

The XRD results

The XRD spectra of the UHMWPE and UHMWPE/SWCNTs nanocomposite are shown in Fig. 6. The results showed a strong intensity reflection peak for UHMWPE at $2\theta = 21°$ and a less intense reflection peak at $2\theta = 23°$, indicating the reflection located at (110), (200) planes, respectively; which are for the orthorhombic unit cell structure [14, 23–25]. Also, three weak peaks indicating the reflection located at (210), (020), and (011) planes were distinguished at $2\theta = 30°$, 36°, and 39°, respectively [26, 27]. The results showed that adding P-SWCNTs and Amide-SWCNTs (1–5 wt %) did not affect the matrix structure. The grain size and grain boundaries affect the mechanical properties of the material. The orthorhombic structure has different crystal orientations as shown in Fig. 5 and thus common grain boundaries. When the amide-SWCNTs were added within the UHMWPE matrix, an increase in the crystallization of UHMWPE and

on the other hand a decrease in the grain size were observed. The explanation for this is that the amide-SWCNTs act as a nucleation agents that changes the nucleation type of UHMWPE from homogeneous nucleation to heterogeneous nucleation, which led to accelerating the nucleation process and the formation of more crystalline grains [14]. This acceleration in the grains' growth explains the decrease in grain size due to the transformation of the structure from coarse grains to fine grains, in which, the smaller the size of the grains (fine-grain), the higher the grain boundaries, which leads to more obstacles to dislocation motion (slip) and high toughness material [28]. This is also noticed as a result in the tensile strength measurements will be discussed later. It was also observed that the largest increase in crystallinity of UHMWPE was when adding 4% Amide-SWC-NTs; which is due to the good dispersion within the UHMWPE matrix compared to the 5% Amide-SWCNTs composite that shows the presence of agglomerates within the UHMWPE matrix as shown in Fig. 4.

The crystal size, space between atomic lattice, and lattice constants (a, b, and c) for the orthorhombic unit cell structure are calculated as shown in the following Table 2. The space between atomic lattices was calculated by using Bragg's equation [29]:

$$2d \sin \theta = n\lambda$$

where d is the space between atomic lattice, n is a positive integer (1, 2, 3, etc.), and θ is the angle of diffraction. The crystal size was calculated by using Scherrer's equation [29]:

$$D = \frac{K\lambda}{\beta \cos \theta}$$

where D is the crystallite size (Å), K is the Scherrer shape factor, λ is the wavelength, β is the full- width-half-maximum (FWHM) value of the peak in radians and θ is the Bragg angle of the (hkl) reflection. The lattice constant was calculated based on an orthorhombic structure as follows [30]:

$$\frac{1}{d2} = \frac{h2}{a2} + \frac{k2}{b2} + \frac{l2}{c2}$$

where d is the space between atomic lattice, (h, k, l) is the orientation of the orthorhombic plane, and (a, b, and c) is the lattice constant.

The full width at half maximum and space between atomic lattice were calculated by using Origin Pro software. The crystallinity of UHMWPE and the nanocomposites were calculated by using Origin Pro software by measuring the area under the peaks (crystal) divided by the total peak area (crystal + amorphous) as follows [29]:

$$X_\mathrm{c} = \frac{A_\mathrm{c}}{A_\mathrm{c} + A_\mathrm{m}}$$

where X_c *is* the crystallinity (%), A_c is the area under the peaks of crystal, and *Am* is the area under the peaks of the amorphous structure.

Fig. 5 SEM images showing the morphology for the prepared nanocomposites sheets of pure UHM- ▶ WPE, UHMWPE/P-SWCNTs, and UHMWPE/Amide-SWCNTs (1–5 wt %) by using ultra-sonication mixing and hot press molding methods, where **a**, **b**: pure UHMWPE, **c**, **d**: UHMWPE/P- SWCNTs, **e**, **f**: UHMWPE/1 wt % Amide-SWCNTs, **g**, **h**: UHMWPE/2 wt % Amide-SWCNTs, **i**, **j** UHMWPE/3 wt % Amide-SWCNTs, **k**, **l**: UHMWPE/4 wt % Amide-SWCNTs, and **m**, **n**: UHMWPE/5 wt % Amide-SWCNTs

The DSC results

The thermal properties of the UHMWPE and nanocomposite were characterized by using DSC. Figure 7 shows heating thermograms for the UHMWPE, P-SWCNTs, and Amide-SWCNTs (1–5 wt %). Table 3 shows the onset temperature, melting temperature, end temperature, the heat of fusion (enthalpy), and percent of crystallinity for UHMWPE. The degree of crystallinity is calculated by comparing the heat of fusion of each sample resulting from the melting endotherm peak with the theoretical heat of fusion of the polymer. The theoretical heat of fusion of pristine UHMWPE polymer is 289 J/g [31]. The results showed little difference in melting temperature between UHMWPE and the nanocomposites. The observed increase in UHMWPE crystallinity is due to the addition of SWCNTs acting as a template for nucleation of the crystalline lamellae of the UHMWPE chains. The maximum increase in crystallinity was with Amide-SWCNTs addition (3–4 wt %). This can be attributed to reason that the amide group achieved high interfacial adhesion within the UHMWPE matrix, which led to the acceleration of the nucleation process and increased crystallization, which is consonant with the XRD results [14, 17]. Also, the slight shift in UHMWPE /Amide UHMWPE melting temperature is attributed to the formation of more stable and saturated crystals at higher temperatures than UHMWPE compared to UHMWPE/Amide-SWCNTs [32].

Tensile test results

The mechanical properties (Young modulus, yield strength, ultimate tensile strength, strain at failure, and toughness) for UHMWPE, UHMWPE/SWCNTs nanocomposites were characterized by using a universal testing machine. Averaged results from five replicates of each sample are summarized in Table 4. Figure 8 shows an engineering stress–strain curve for pure UHMWPE and UHMWPE/SWCNTs nanocomposites. It is noted that an enhancement in the strain at failure for UHMWPE with the addition of Amide-SWCNTs; this indicates that the Amide group achieved good interfacial adhesion compared to P-SWCNTs. The decrease in the strain at failure when P- SWCNTs were added was due to agglomeration formation within the polymer matrix. This is since the Amide group reduced the aggregation of the SWCNTs resulting from the Vander walls forces and improved the interfacial adhesion, thus enhancing the dispersion of the SWCNTs within the polymer matrix. The maximum enhancement in the strain at failure was (~77%) when adding 4 wt % Amide-SWCNTs compared to P-SWCNTs (-21%). The stiffness increases when adding P-SWCNTs and
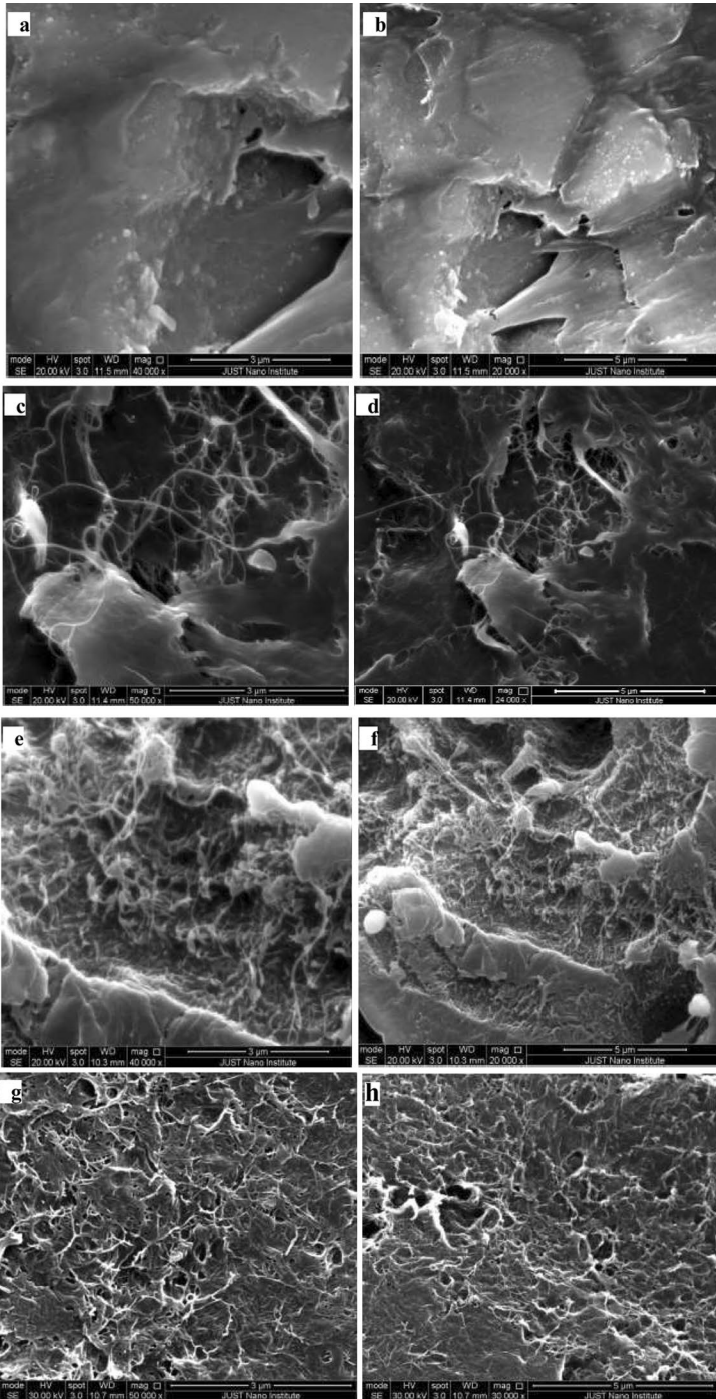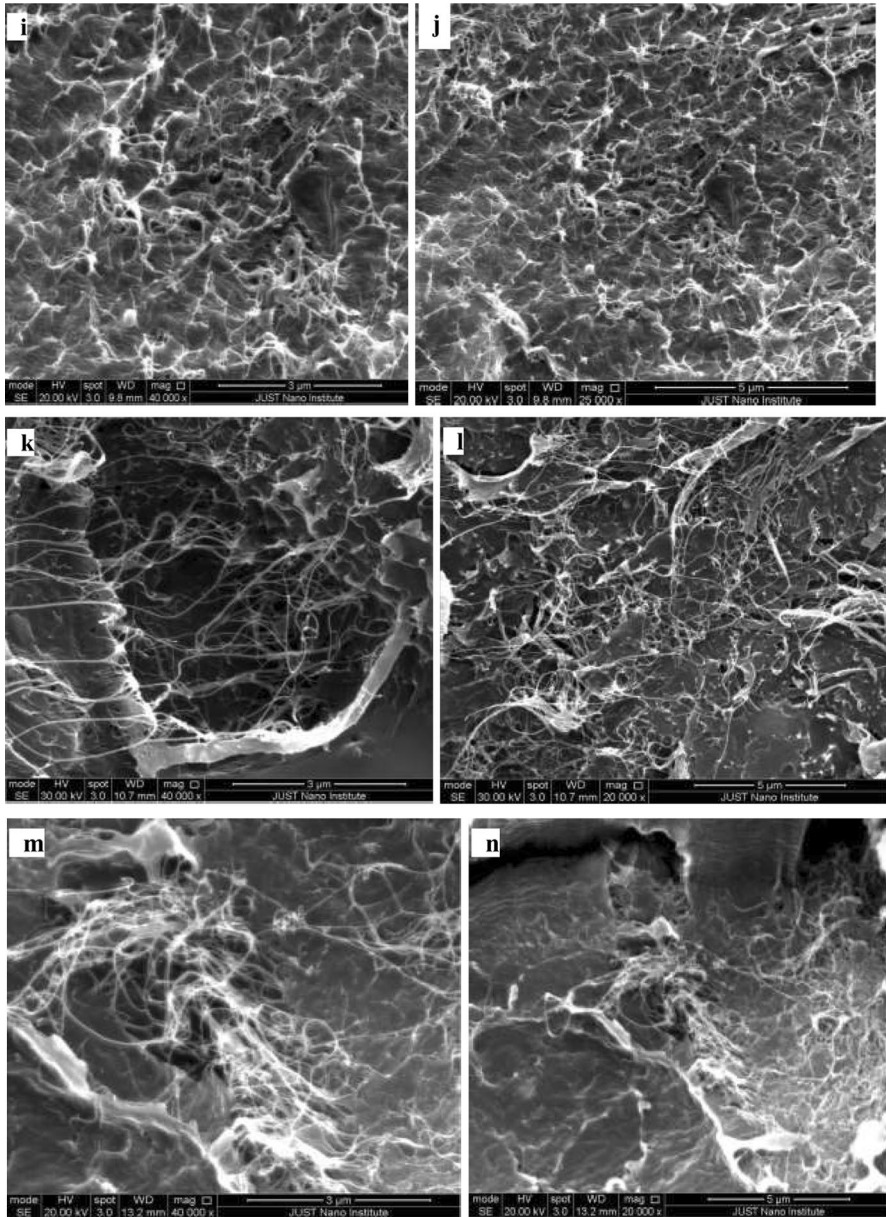
Fig. 5 (continued)

Amide-SWCNTs (1–5 wt %). The maximum enhancement in the ultimate tensile strength was (26.64 MPa) when adding 4 wt % Amide-SWCNTs compared to UHMWPE (22.13 MPa). The enhancement in toughness when adding Amide-SWCNTs (1–5 wt %) was due to the transformation of the structure from coarse
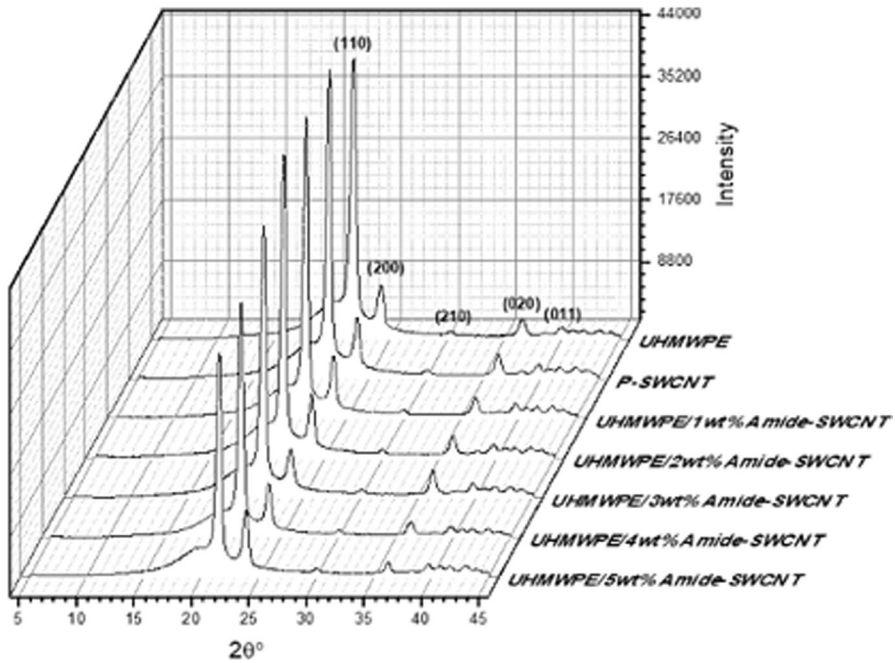
Fig. 6 XRD spectra of the UHMWPE and UHMWPE/SWCNTs nanocomposite

grains to fine grains, thus, creating more grain boundaries. This can lead to more obstacles to the dislocation motion (slip) and high toughness material [28]. This optimization is consistent with the obtained results from the XRD measurements. These results are different from some other studies, the difference came from different factors such as using UHMWPE with different molecular weight values [17], using different processing and preparation methods [17, 18], and different thickness of the tested nanocomposites [33, 34].

The Amide group's addition had an apparent effect on improving the crystallinity and the mechanical properties of the UHMWPE. This is related to the Amide group ability to reduce the aggregation of the SWCNTs resulting from the Vander walls forces and improved the interfacial adhesion, thus enhancing the dispersion of the SWCNTs within the polymer matrix, which led to the improvement of the load transfer efficiency applied to the composite. Adding P-SWCNTs and Amide-SWCNTs (1–5 wt %) did not affect the matrix structure (orthorhombic structure). The addition of the Amide-SWCNTs improved the degree of crystallinity due to changing the nucleation type of UHMWPE from the homogeneous to the heterogeneous nucleation, which led to accelerating the nucleation process and the formation of more crystalline grains. This acceleration in the grain growth explains the decrease in the grain size due to the transformed structure from coarse grains to fine grains, thus creating more grain boundary, which leads to more obstacles to dislocation motion (slip) and high toughness material.

Table 2 Crystallinity, crystal size, space between atomic lattice, and lattice constant (a, b, and c) for the UHMWPE and UHMWPE/SWCNTs nanocomposites

Sample	% of SWCNTs	Nanocomposite	Crystallinity %	Change (%)	Crystal size (Å)	Miller indices	d-spacing (Å)	Lattice constant (Å)
S1	–	UHMWPE	67.75	–	169	(110)	4.081	$a = 7.358$
						(200)	3.679	$b = 4.904$
						(020)	2.964	$c = 2.539$
						(210)	2.462	
						(011)	2.254	
S2	1	UHMWPE/P-SWCNTs	74.47	+10	170	(110)	4.118	$a = 7.425$
						(200)	3.712	$b = 4.949$
						(020)	2.969	$c = 2.547$
						(210)	2.474	
						(011)	2.265	
S3	1	UHMWPE/1 wt % Amide-SWCNTs	74.73	+10	166	(110)	4.141	$a = 7.465$
						(200)	3.732	$b = 4.977$
						(020)	2.796	$c = 2.551$
						(210)	2.480	
						(011)	2.270	
S4	2	UHMWPE/2 wt % Amide-SWCNTs	76.05	+12	168	(110)	4.143	$a = 7.458$
						(200)	3.729	$b = 4.982$
						(020)	2.976	$c = 2.551$
						(210)	2.482	
						(011)	2.271	
S5	3	UHMWPE/3 wt % Amide-SWCNTs	75.58	+11	157	(110)	4.114	$a = 7.434$
						(200)	3.717	$b = 4.940$
						(020)	2.969	$c = 2.546$
						(210)	2.470	
						(011)	2.263	

Table 2 (continued)

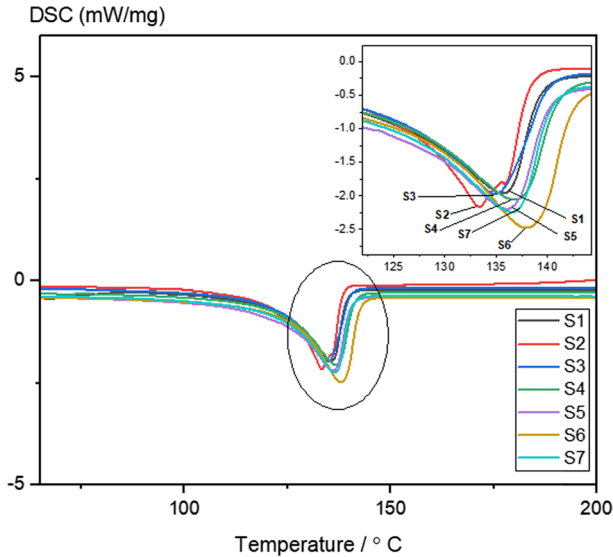| Sample	% of SWCNTs	Nanocomposite	Crystallinity %	Change (%)	Crystal size (Å)	Miller indices	d-spacing (Å)	Lattice constant (Å)
S6	4	UHMWPE/4 wt	78.27	+16	158	(110)	4.120	a=7.431
		% Amide-				(200)	3.715	b=4.951
		SWCNTs				(020)	2.969	c=2.547
						(210)	2.474	
						(011)	2.265	
S7	5	UHMWPE/5 wt	74.9	+11	161	(110)	4.135	a=7.455
		% Amide-				(200)	3.727	b=4.970
		SWCNTs				(020)	2.969	c=2.550
						(210)	2.478	
						(011)	2.269	

Fig. 7 DSC heating endotherms of UHMWPE and UHMWPE nanocomposite

Table 3 DSC data from heating thermograms of UHMWPE, P-SWCNTs, and Amide-SWCNTs (1–5 wt%)

Material	T(on) °C	Tm °C	Tf °C	Heat of fusion J/g	Crystallinity %
S1	125.1	135.7	139.2	191.66	66.32
S2	126.2	135.4	138.2	219.26	75.87
S3	126.1	135.3	139.3	217.45	75.25
S4	126.9	136.9	141	221.02	76.48
S5	126.3	135.9	140.1	223.13	77.21
S6	128.4	138.1	142.3	229.2	79.31
S7	126.1	136.6	140.2	211.63	73.23

Table 4 Mechanical properties of UHMWPE and UHMWPE/SWCNT nanocomposite based on the tensile test results

| Sample name	Young modulus (MPa)	Yield strength (MPa)	Ultimate tensile strength (MPa)	Strain at failure (mm/mm)	Toughness (MJ/m^3)
S1	328.80 ± 20.67	18.51 ± 1.99	22.13 ± 3.88	0.823 ± 0.17	16.55 ± 4.41
S2	393.96 ± 10.83	19.17 ± 1.20	23.6 ± 4.04	0.65 ± 0.19	14.11 ± 1.77
S3	351.19 ± 37.02	18.28 ± 1.54	23.29 ± 2.32	1.16 ± 0.11	23.86 ± 3.34
S4	384.68 ± 23.00	18.79 ± 1.33	24.04 ± 1.99	1.16 ± 0.21	24.43 ± 4.14
S5	403.45 ± 33.77	20.09 ± 2.00	24.18 ± 2.88	1.10 ± 0.23	24.05 ± 2.56
S6	391.20 ± 22.10	19.05 ± 1.87	26.64 ± 1.55	1.46 ± 0.15	32.36 ± 2.43
S7	360.35 ± 40.21	19.46 ± 1.43	24.83 ± 3.46	1.18 ± 0.10	25.82 ± 3.67
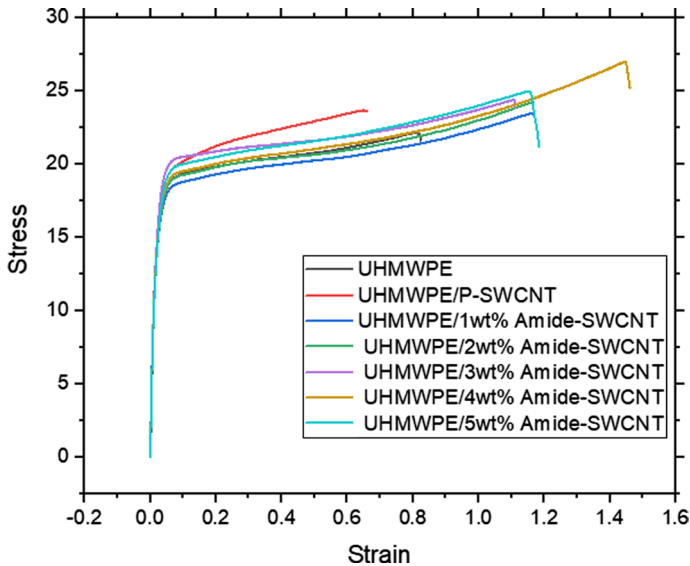
Fig. 8 Stress–strain curve for UHMWPE and UHMWPE/SWCNTs nanocomposites

Conclusion

UHMWPE/Amide-SWCNTs nanocomposites sheets were successfully prepared by using combined preparation methods; ultra-sonication with hot press molding. Functionalization of the SWCNTs with Amide group has improved the interfacial adhesion between UHMWPE polymer matrix and the Amide-SWCNTs. Characterization showed that the prepared nanocomposites were with improved crystallinity and mechanical properties in comparison with pristine UHMWPE polymer. Addition of P-SWCNTs 1% or Amide-SWCNTs (1–5 wt %) did not change the crystal structure of the UHMWPE (orthorhombic structure). However, addition of 4 wt % Amide-SWCNTs improved the degree of crystallinity up to 16% due to changing in the nucleation type of UHMWPE from homogeneous to heterogeneous nucleation. Effects of the combined preparation methods and the functionalization of the SWCNTs were clearly revealed in the mechanical properties of the nanocomposites comparing to the pristine polymer. Young's modulus, tensile strength, strain at failure, and toughness were improved when adding 4 wt % Amide-SWCNTs up to 19%, 20%, 77%, and 95%, respectively. The Amide group increases the degree of dispersion of the nanofiller within the polymer matrix which maximizes the effective interfacial adhesion compared to pristine SWCNTs.

References

1. Loste J, Lopez-Cuesta JM, Billon L, Garay H, Save M (2019) Transparent polymer nanocomposites: an overview on their synthesis and advanced properties. Prog Polym Sci 89:133–158

2. Sobieraj MC, Rimnac CM (2009) Ultra high molecular weight polyethylene: mechanics, morphology, and clinical behavior. J Mech Behav Biomed Mater 2(5):433–443. https://doi.org/10.1016/j.jmbbm.2008.12.006

3. Hussain M, Naqvi RA, Abbas N, Khan SM, Nawaz S, Hussain A, Zahra N, Khalid MW (2020) Ultra-high-molecular-weight-polyethylene (UHMWPE) as a promising polymer material for biomedical applications: a concise review. Polymers 12(2):1–28. https://doi.org/10.3390/polym12020323

4. Choudhary V, Singh BP, Mathur RB (2013) Carbon nanotubes and their composites. Syntheses Appl Carbon Nanotubes Composites. https://doi.org/10.5772/52897

5. Fredriksson T (2014) Carbon nanotubes: a theoretical study of Young's modulus

6. Lau KY, Piah MAM (2011) Polymer nanocomposites in high voltage electrical insulation perspective: a review. Malays Polym J 6(1):58–69

7. Dao NN, Luu MD, Nguyen QK, Kim BS (2011) UV absorption by cerium oxide nanoparticles/epoxy composite thin films. Adv Nat Sci Nanosci Nanotechnol 2(4):4–8

8. Wang W, Zhang B, Jiang S, Bai H, Zhang S (2019) Use of CeO2 nanoparticles to enhance UV-shielding of transparent regenerated cellulose films. Polymers (Basel) 11(3)

9. Crosby AJ, Lee JY (2007) Polymer nanocomposites: the 'nano' effect on mechanical properties. Polym Rev 47(2):217–229

10. Ma PC, Siddiqui NA, Marom G, Kim JK (2010) Dispersion and functionalization of carbon nanotubes for polymer-based nanocomposites: a review. Compos Part A Appl Sci Manuf 41(10):1345–1367

11. Outline C (2015) Fundamentals of polymer matrix composites containing CNTs

12. Zhang J, Zou H, Qing Q, Yang Y, Li Q, Liu Z, Guo X, Du Z (2013) Effect of chemical oxidation on the structure of single-walled carbon nanotubes. J Phys Chem Part B 107(16):3712–3718

13. Gromov A, Dittmer S, Svensson J, Nerushev OA, Perez-García SA, Licea-Jiménez L et al (2005) Covalent amino-functionalisation of single-wall carbon nanotubes. J Mater Chem 15(32):3334–3339

14. Guo C, Sun F, Ling R, Yao J, Zhang Z, Zhang G (2016) Crystallization and stress relaxation behaviors of UHMWPE/CNT fibers. J Vinyl Addit Technol 24(3):229–232

15. Grady BP, Arthur DJ, Ferguson J (2009) Single-walled carbon nanotube/ultrahigh-molecular-weight polyethylene composites with percolation at low nanotube contents. Polym Eng Sci 49(12):2440–2446

16. Khatiwada S, Armada CA, Barrera EV (2013) Hypervelocity impact experiments on epoxy/ultra high molecular weight polyethylene fiber composites reinforced with single- walled carbon nanotubes. Procedia Eng. 58:4–10. https://doi.org/10.1016/j.proeng.2013.05.003

17. Hulsey S, Absar S, Sultan QN, Sabet SM, Mahfuz H, Khan M (2018) Synthesis and characterization of UHMWPE nanocomposite fibers containing carbon nanotubes coated with a PVP surfactant layer. Polymer Composites-. https://doi.org/10.1002/pc,E1025-E1033

18. Khan MR, Mahfuz H, Adnan A, Shabib I, Leventouri T (2013) Elastic properties of UHMWPE-SWCNT nanocomposites' fiber: an experimental, theoretic, and molecular dynamics evaluation. J Mater Eng Perform 22(6):1593–1600

19. Arrigo R, Teresi R, Gambarotti C, Parisi F, Lazzara G, Dintcheva NT (2018) Sonication-induced modification of carbon nanotubes: effect on the rheological and thermo-oxidative behaviour of polymer-based nanocomposites. Materials (Basel) 11(3):1–14

20. Atieh MA, Bakather OY, Al-Tawbini B, Bukhari AA, Abuilaiwi FA, Fettouhi MB (2010) Effect of carboxylic functional group functionalized on carbon nanotubes surface on the removal of lead from water. Bioinorg Chem Appl

21. Abuilaiwi FA, Laoui T, Al-Harthi M, Atieh MA (2010) Modification and functionalization of multiwalled carbon nanotube (MWCNT) via fischer esterification. Arab J Sci Eng. 35(1 C):37–48

22. Azizian J, Tahermansouri H, Biazar E, Heidari S, Khoei DC (2010) Functionalization of carboxylated multiwall nanotubes with imidazole derivatives and their toxicity investigations. Int J Nanomed 5(1):907–914

23. Trujillo M, Arnal ML, Müller AJ, Laredo E, Bredeau S, Bonduel D et al (2007) Thermal and morphological characterization of nanocomposites prepared by in-situ polymerization of high-density polyethylene on carbon nanotubes. Macromolecules 40(17):6268–6276

24. Wang X, Zheng H, Sun Y (2018) Study on structures and properties of ultra-hot drawing UHMWPE fibers fabricated via dry spinning method. J Polym Eng 38(9):863–870

25. Ghasemi H, Thoppey N, Huang X, Loomis J, Li X, Tong J, et al (2014) High thermal conductivity ultra-high molecular weight polyethylene (UHMWPE) films. In: Intersociety conference on thermal and thermomechanical phenomena in electronic systems 235–9

26. Fontana L, Vinh DQ, Santoro M, Scandolo S, Gorelli FA, Bini R et al (2007) High-pressure crystalline polyethylene studied by x-ray diffraction and ab initio simulations. Phys Rev B Condens Matter Mater Phys 75(17):1–11

27. Chouit F, Guellati O, Boukhezar S, Harat A, Guerioune M, Badi N (2014) Synthesis and characterization of HDPE/N-MWNT nanocomposite films. Nanoscale Res Lett 9(1):1–6

28. Smith E (1985) Dislocations and fracture (August):205–20

29. To P.S. Chapter 7 : Basics of X-ray Diffraction. Solutions. 1–25. From http://epswww.unm.edu/xrd/xrdbasics.pdf. 1999.

30. Du M, Cui L, Liu F (2019) A new reversible phase transformation of intermetallic Ti3Sn. Materials (Basel) 12(15):6–15

31. Enqvist E (2013) Evelina enqvist carbon nanofiller reinforced UHMWPE for orthopaedic applications optimization of manufacturing parameters

32. Vega JF, Fernández-Alcázar J, López JV, Michell RM, Pérez-Camargo RA, Ruelle B et al (2017) Competition between supernucleation and plasticization in the crystallization and rheological behavior of PCL/CNT-based nanocomposites and nanohybrids. J Polym Sci Part B Polym Phys 55(17):1310–1325

33. Bakshi SR, Tercero JE, Agarwal A (2007) Synthesis and characterization of multiwalled carbon nanotube reinforced ultra high molecular weight polyethylene composite by electrostatic spraying technique. Compos Part A Appl Sci Manuf 38(12):2493–2499

34. Ruan SL, Gao P, Yang XG, Yu TX (2003) Toughening high performance ultrahigh molecular weight polyethylene using multiwalled carbon nanotubes. Polymer (Guildf) 44(19):5643–5654